

## Antiproliferative Gold(I) Complexes

## Sugar-Incorporated N-Heterocyclic-Carbene-Containing Gold(I) Complexes: Synthesis, Characterization, and Cytotoxic Evaluation

Maria E. Cucciolito,<sup>[a,b]</sup> Marina Trinchillo,<sup>[a]</sup> Roberta Iannitti,<sup>[c]</sup> Rosanna Palumbo,<sup>[c]</sup> Diego Tesauro,<sup>[d,e]</sup> Angela Tuzi,<sup>[a]</sup> Francesco Ruffo,<sup>[a,b]</sup> and Angela D'Amora<sup>\*[a,e]</sup>

**Abstract:** A series of neutral and cationic gold(I) complexes bearing a glucopyranoside-incorporated N-heterocyclic carbene (NHC) ligand are synthesized and structurally characterized. Different secondary ligands (chlorido, phosphane, or sugar-NHC) are employed to tune the properties of the complexes. The antiproliferative effects of the compounds are evaluated against

PC-3 prostate cancer cells and a panel of human tumor cell lines. The activities of the phosphane complexes are comparable to that observed for cisplatin. The combined results provide further insights into the biological behavior of NHC-gold complexes.

## Introduction

Although cisplatin (CDDP) is a successful chemotherapeutic drug for many oncological pathologies and was first approved by the U.S. Food and Drug Administration (FDA) in 1978 for the treatment of genitourinary tumors, it shows side-effects and resistance can occur during the care process.<sup>[1]</sup> Therefore, the scientific community has been engaged in the search for new transition-metal complexes that can act as growth-inhibiting agents towards tumor cells.<sup>[2]</sup> Among the non-platinum antitumor agents, gold complexes have gained increasing attention owing to their strong antiproliferative effects, which generally occur through non-cisplatin-like mechanisms of action, as well as their pharmacodynamic and pharmacokinetic properties.<sup>[3]</sup> The first gold complex approved by the FDA in 1985 was {[2,3,4,6-tetra-O-acetyl-1-(thio-κS)-β-D-glucopyranosato]-(triethylphosphane)gold(I)} (auranofin), which is used clinically as an antiarthritis agent.<sup>[4]</sup> At the end of 2016, phase I and II clinical studies of this compound for the treatment of chronic

lymphocytic leukemia (CLL) were completed.<sup>[5]</sup> The successful application of auranofin in medical treatments in the last decade prompted researchers to test two-coordinate gold(I) complexes as antibacterial and cytotoxic agents.<sup>[6]</sup> The stability of the complexes in vivo as well as their lipophilicities, hydrophilicities, and redox properties can be tuned by the choice of auxiliary ligands. Ligands able to stabilize the gold(I) center include phosphanes,<sup>[6]</sup> thiolates,<sup>[7]</sup> and N-heterocyclic carbenes (NHCs).<sup>[8]</sup> Within this framework, NHC-gold complexes provide the most promise, and several neutral and cationic gold carbene species have been prepared and characterized in the last few years.<sup>[8b,9,10]</sup> The mechanism of action of these compounds is still highly debated, and recent studies<sup>[11–14]</sup> support the view that gold carbene complexes work through the metalation of many proteins bearing specific structural motifs for metal recognition.

The decoration of the imidazole ring of the NHC with biologically active residues or the conjugation of the NHC-Au<sup>I</sup> species with specific aptamers enhances the activity of the complexes.<sup>[14,15]</sup> In addition, carbohydrate uptake is significantly increased in cancer cells; therefore, the design of glycoconjugates has become an appealing strategy for the targeted delivery of anticancer drugs.<sup>[16,17]</sup> Furthermore, the chemical properties of carbohydrates are very attractive as a wide variety of substituents can be introduced<sup>[18]</sup> and multiple interaction points for H-bond donors or acceptors can be provided.

Inspired by all of these considerations, we investigated the design and the synthesis of four gold(I) complexes (Figure 1) containing the sugar-incorporated NHC ligand 1-methyl-3-(2,3,4,6-tetra-O-acetyl-β-D-glucopyranosyl)imidazolene (magi).

The cytotoxic properties of all of the compounds were screened against PC-3 prostate cancer cells. The most promising compound, [magiAuP1][BF<sub>4</sub>], was tested against a panel of human tumor cell lines.

[a] Dipartimento di Scienze Chimiche, Università degli Studi di Napoli Federico II, Complesso Universitario di Monte S. Angelo, Via Cintia 21, 80126 Napoli, Italy  
E-mail: angela.damora@unina.it

[b] Consorzio Interuniversitario di Reattività Chimica e Catalisi, Via Celso Ulpiani 27, 70126 Bari, Italy

[c] Istituto di Biostrutture e Bioimmagini (IBB) CNR, Via Mezzocannone 16, 80134 Napoli, Italy

[d] Dipartimento di Farmacia & CIRPeB Università degli Studi di Napoli Federico II, Via Mezzocannone 16, 80134 Napoli, Italy

[e] Diagnostica e Farmaceutica Molecolari S.C.R.L. (DFM), Via Mezzocannone 16, 80134 Napoli, Italy

Supporting information and ORCID(s) from the author(s) for this article are available on the WWW under <https://doi.org/10.1002/ejic.201700768>.

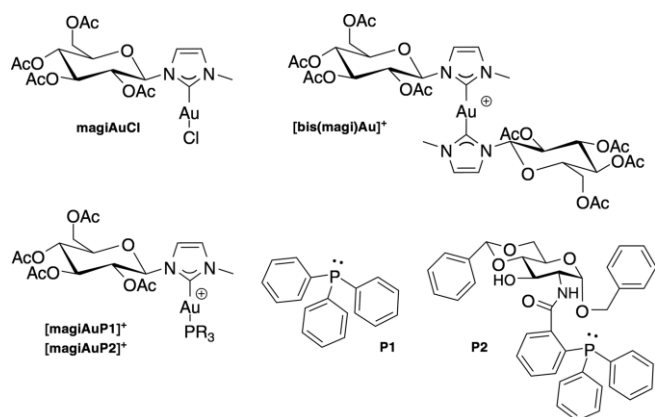
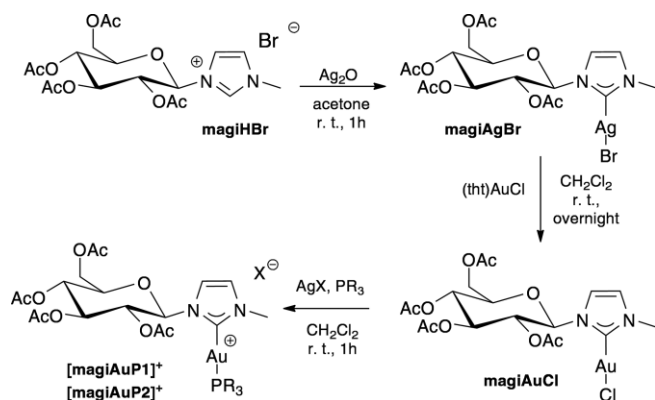


Figure 1. Structures of magi–Au<sup>I</sup> complexes.

## Results and Discussion

### Synthesis of Gold(I) Complexes

The synthesis of the gold(I) complex [magiAuCl] was performed through the known transmetalation route with the corresponding Ag<sup>I</sup> complex, which was prepared according to the general method described by Nishioka et al.,<sup>[19]</sup> and the transfer of the magi ligand to the Au<sup>I</sup> precursor [(tth)AuCl] (tth = tetrahydrothiophene, Scheme 1).



Scheme 1. Synthesis of the Au<sup>I</sup> complexes [magiAuCl], [magiAuP1]BF<sub>4</sub>, and [magiAuP2][OSO<sub>2</sub>CF<sub>3</sub>].

The complex [magiAuCl] was isolated in 90 % yield and characterized through <sup>1</sup>H and <sup>13</sup>C{<sup>1</sup>H} NMR spectroscopy. In the <sup>13</sup>C{<sup>1</sup>H} NMR spectrum, a significant shift was observed for the signal corresponding to the carbene carbon atom, which moved from  $\delta = 139$  ppm for the imidazolium salt to  $\delta = 172.4$  ppm.<sup>[20]</sup>

Crystals of [magiAuCl] suitable for XRD were obtained through the slow evaporation of a solution of the complex in *N,N*-dimethylformamide (DMF) at room temperature. The X-ray diffraction study confirmed the identity of the compound as a neutral mononuclear NHC–Au<sup>I</sup> complex (Figure 2). The compound crystallizes in the monoclinic *P*<sub>2</sub><sub>1</sub> space group with one molecule of the complex and one solvate DMF molecule in the independent unit.

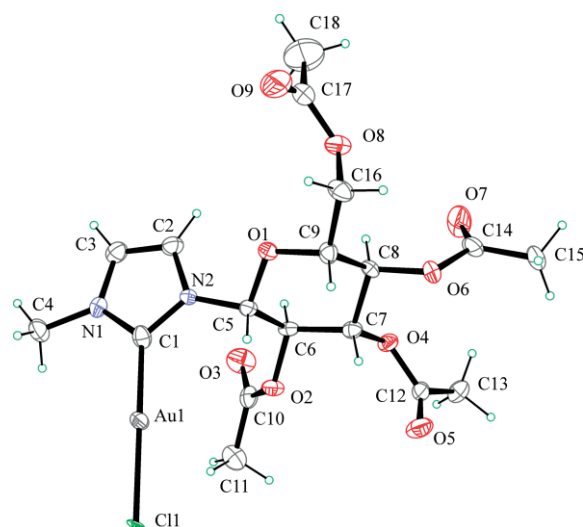


Figure 2. ORTEP view of [magiAuCl]. Thermal ellipsoids are drawn at the 50 % probability level. Selected bond lengths [Å] and angles [°]: Au1–C1 2.3209(12), Au1–Cl 1.943(8); C1–Au1–Cl 176.8(5).

All of the bond lengths and angles in the NHC ligand are in the normal ranges. The crystal data and structure details are reported in the Supporting Information (Table S1). The Au–Cl and Au–C bond lengths are consistent with those of analogous (NHC)AuCl compounds.<sup>[21]</sup> As expected, the Au atom is linearly two-coordinate and bonded to the central carbon atom of the NHC ligand and the chlorine atom. The encumbered pendant pyranose ring in the complex is in the chair conformation with all substituents in equatorial positions. The ring is almost perpendicular to the imidazole plane to interact favorably with the metal center. In the crystal packing, one interesting feature is the presence of intra- and intermolecular Au...HC<sub>methyl</sub> contacts that assemble the molecules into columns running along the *b* axis (Figures S1 and S2). No aurophilic interactions were found, and the shortest intermolecular Au1...Au1 distance is 6.734(1) Å.

The two cationic carbene complexes [magiAuP1][BF<sub>4</sub>] and [magiAuP2][OSO<sub>2</sub>CF<sub>3</sub>] (Scheme 1), were synthesized by replacing the chlorido ligand with triphenylphosphane (P1) or the glycosylated phosphane P2.<sup>[22]</sup> The procedure reported by Casini was adapted;<sup>[2]</sup> the neutral complex [magiAuCl] was dissolved in dichloromethane at room temperature, and the appropriate amount of the phosphane ligand and a slight excess of the silver salt as a halide abstractor were added. After the partial evaporation of the CH<sub>2</sub>Cl<sub>2</sub>, the new cationic gold complexes [magiAuP1][BF<sub>4</sub>] and [magiAuP2][OSO<sub>2</sub>CF<sub>3</sub>] were precipitated with diethyl ether and isolated in high yields (up to 90 %). In the NMR spectrum, the resonances of the sugar protons were assigned on the basis of both their expected chemical shifts and the coupling constants within the glucose ring. The <sup>31</sup>P{<sup>1</sup>H} NMR spectra of [magiAuP1][BF<sub>4</sub>] and [magiAuP2][OSO<sub>2</sub>CF<sub>3</sub>] showed one broad singlet at  $\delta = 40.2$  and 40.4 ppm, respectively, which are diagnostic of cationic gold(I)–phosphane complexes.<sup>[23]</sup> Finally, the <sup>13</sup>C{<sup>1</sup>H} NMR spectra display the characteristic signals of the carbene carbon atom bound to a cationic gold(I) center at  $\delta \approx 185$  ppm, which is shifted downfield by

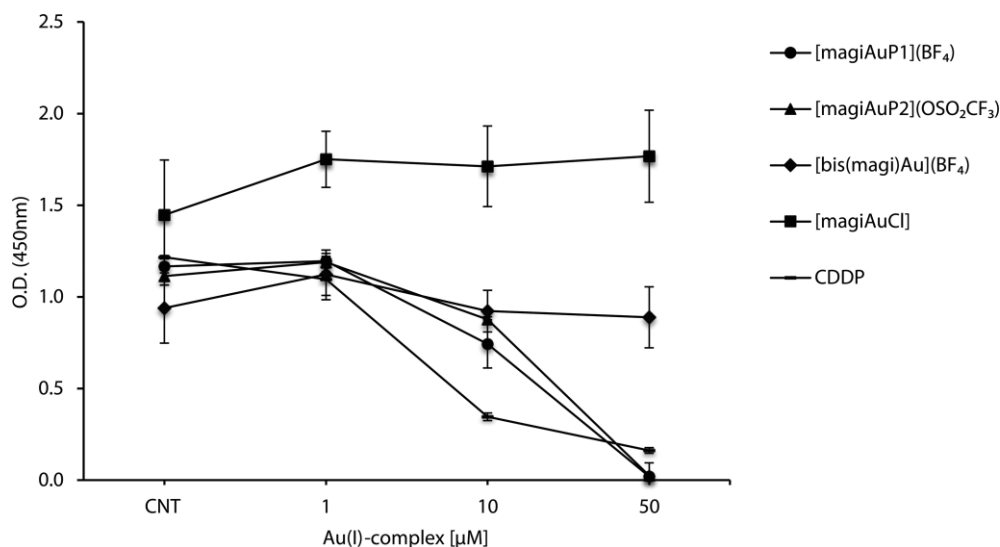
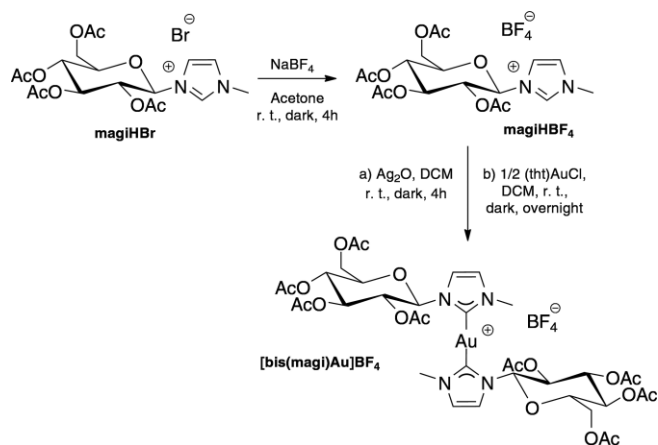


Figure 3. Effect of Au<sup>I</sup> complexes and cisplatin on the total metabolic activity of PC-3 cancer cells. The PC-3 cells ( $4 \times 10^3$ ) were seeded in 96-well plates and treated with different concentrations of the Au<sup>I</sup> complexes for 72 h. After the treatment, CCK-8 assays were performed. [magiAuP1]BF<sub>4</sub> and [magiAuP2][OSO<sub>2</sub>CF<sub>3</sub>] reduced the metabolic activity in a dose-dependent manner, whereas [magiAuCl] and [bis(magi)Au]BF<sub>4</sub> showed no significant activity. Cells treated with DMSO (0.1 %) and cisplatin (CDDP) were included for control and comparative purposes respectively [ $n = 3$ , the standard deviations (SDs) are indicated].

ca. 10–15 ppm with respect to that of halide complexes.<sup>[21a]</sup> Furthermore, <sup>19</sup>F NMR spectra were collected for both complexes.

The treatment of a CH<sub>2</sub>Cl<sub>2</sub> solution of the imidazolium salt magiHBF<sub>4</sub> containing a non-coordinating anion with silver oxide and then (tht)AuCl resulted in the formation of [bis(magi)Au<sup>I</sup>][BF<sub>4</sub>] in good yield (Scheme 2).<sup>[24]</sup>



Scheme 2. Synthesis of the bis(NHC)Au<sup>I</sup> complex [bis(magi)Au][BF<sub>4</sub>].

The observance of only one set of NHC signals in the <sup>1</sup>H NMR spectrum of [bis(magi)Au][BF<sub>4</sub>] indicates a symmetric structure, whereas the most diagnostic feature in the <sup>13</sup>C{<sup>1</sup>H} NMR spectrum is the signal at  $\delta = 182.9$  ppm, which is indicative of an NHC–Au<sup>I</sup> bond.<sup>[25]</sup>

### Cytotoxicity Assays

To investigate the abilities of the NHC–Au<sup>I</sup> complexes to the inhibit growth of prostate cancer cells, used as a metastatic

model, increasing amounts of complexes were added to a cell-culture medium. Cisplatin and magiHBr were used as comparative compounds (Figure 3; Table 1). At the tested concentrations, the free ligand was totally inert. The decreased proliferation of PC-3 cells was obtained after treatment with 10  $\mu$ M of [magiAuP1]BF<sub>4</sub> or [magiAuP<sub>2</sub>][OSO<sub>2</sub>CF<sub>3</sub>] (by ca. 40 and 30 %, respectively; Figure 3). Under the same experimental conditions, the compounds that do not contain phosphanes showed half-maximal effective concentration (EC<sub>50</sub>) values more than ten times higher (Table 1).

Table 1. EC<sub>50</sub> values of the Au<sup>I</sup> complexes against PC-3 cell lines.

Au <sup>I</sup> complex	EC <sub>50</sub> [ $\mu$ M] <sup>[a]</sup>
magiHBr	>300 $\pm$ 0.2
[magiAuP1]BF <sub>4</sub>	9.0 $\pm$ 0.06
[magiAuP2][OSO <sub>2</sub> CF <sub>3</sub> ]	10.0 $\pm$ 0.07
[magiAuCl]	100 $\pm$ 0.19
[bis(magi)Au]BF <sub>4</sub>	>100 $\pm$ 0.06

[a] Average of three independent experiments, SDs determined by crystal violet assays (72 h incubation time). Solutions of the Au<sup>I</sup> complexes were prepared through the dilution of freshly prepared stock solutions ( $10^{-2}$  M in DMSO) of the compounds in culture medium.

The introduction of the sugar function to the phosphane ligand did not affect the cytotoxic activity. This result provides further evidence that this auxiliary ligand is substituted by Lewis bases of the molecular cellular target. The neutral chlorido complex did not have a significant effect on tumor-cell growth.

Generally, in a similar series of carbene complexes, the EC<sub>50</sub> values of cationic species are one order of magnitude smaller than those of neutral complexes. The higher antiproliferative effect is attributed to the presence of the positive charge combined with the rather large lipophilic character of NHC ligands. The dramatic effect of the charge observed in this study suggests that the cationic complexes are not neutralized in the

physiological environment and also that the lack of activity for the neutral complexes can be attributed to poor mitochondrial penetration.

The inertness<sup>[26]</sup> of [bis(magi)Au]BF<sub>4</sub> can be explained on the same basis, if it is assumed that the pathway to the mitochondrial target is similarly hindered. In a previous study,<sup>[11d]</sup> these species were more reactive toward the fundamental interaction with Thx (Thx = thioredoxin reductase).

Moreover, the antiproliferative effect of [magiAuP1]BF<sub>4</sub> was investigated against a panel of human cancer cells. As shown in Table 2, the concentration to achieve a 50 % reduction in the fold extent of proliferation was similar for all tested cell lines.

Table 2. Growth inhibition of [magiAuP1]BF<sub>4</sub> and cisplatin against different cell lines.

	EC50 [μM] <sup>[a]</sup>			
	PC-3	A375	U2OS	MCF7
[magiAuP1]BF <sub>4</sub>	9 ± 0.06	10 ± 0.15	10 ± 0.05	14 ± 0.1
cisplatin	6 ± 0.03	6 ± 0.05	n.d.	5.7 ± 0.02

[a] Average of three independent experiments, SD determined by crystal violet assay (72 h incubation time); n.d., not determined.

A comparison of the cytotoxic activities of these sugar–carbene gold complexes with those of similar sugar-containing moieties reported previously shows a general lower activity.<sup>[14b]</sup> These results allow us to ascribe the nanomolar EC50 value for the sugar–carbene complex of the Tamm group to the triazole-tethered function.

Furthermore, cells treated with 10 μM [magiAuP1]BF<sub>4</sub> and assessed by western blot failed to show a cleavage of poly(ADP-ribose) polymerase, a classical hallmark of apoptosis (data not shown). Lactate dehydrogenase (LDH) is a stable enzyme present in all cell types, and the appearance of this protein in the extracellular milieu is a conventional marker for the loss of membrane integrity and the presence of necrosis. For this purpose, LDH release was assessed in PC-3 cells treated with different concentrations of [magiAuP1]BF<sub>4</sub> for 72 h. As shown in Figure 4, a significant increase by ca. 50 % was observed in cells incubated with 10 μM [magiAuP1]BF<sub>4</sub>.

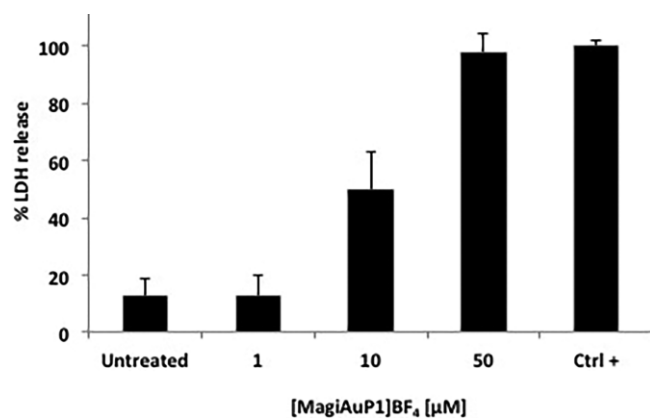


Figure 4. LDH release in PC-3 cells treated with various concentrations of [magiAuP1]BF<sub>4</sub> for 72 h. Treatment with 0.1 % triton for 1 h is included as positive control. Each point represents the mean ± SD of two experiments performed in triplicate.

These results taken together suggest that cells treated with [magiAuP1]BF<sub>4</sub> undergo necrosis, which cannot be considered only as a passive and accidental form of cell death but a programmed event, as indicated in many recent studies.<sup>[27]</sup>

## Conclusions

A series of neutral and cationic sugar-incorporated NHC gold(I) complexes with Cl, magi NHC, or phosphanes as the second ligand were synthesized and thoroughly characterized by spectroscopic methods. The structure of magiAuCl was also solved by X-ray diffraction. All of the compounds were investigated biologically against PC-3 prostate cancer cells, and [magiAuP1]BF<sub>4</sub> was tested against a panel of human tumor cell lines. Both phosphane complexes, [magiAuP2][OSO<sub>2</sub>CF<sub>3</sub>] and [magiAuP1]BF<sub>4</sub>, have comparable EC50 values to that of cisplatin, whereas the neutral complex is totally inactive. Unexpectedly, the cationic biscarbene sugar-based complex [bis(magi)Au]BF<sub>4</sub> is also inert.

The dramatic effects of both charge and auxiliary ligands as well as literature data for Au<sup>I</sup>–carbene species show that the interactions with biomolecules can be affected strongly by the substituents of the imidazole moiety even for systems with similar electronic and lipophilic properties.

## Experimental Section

**Materials and General Methods:** All reagents and solvents were obtained from commercial sources and used without any further purification. The products were characterized by <sup>1</sup>H, <sup>19</sup>F, <sup>31</sup>P, and <sup>13</sup>C NMR spectroscopy. The spectra were recorded with Bruker AVANCE 400 and Varian Inova 500 spectrometers, and the signals are relative to tetramethylsilane (TMS, <sup>1</sup>H and <sup>13</sup>C), CCl<sub>3</sub>F (<sup>19</sup>F), and H<sub>3</sub>PO<sub>4</sub> (<sup>31</sup>P). All coupling constants *J* are quoted in Hz. The elemental analyses were performed with a Carlo Erba 1106 elemental analyzer. HAuCl<sub>4</sub>, THT, 1-methylimidazole, AgBF<sub>4</sub>, AgOSO<sub>2</sub>CF<sub>3</sub>, and Ag<sub>2</sub>O were purchased from Sigma–Aldrich. Ligand P2,<sup>[22]</sup> (tHt)AuCl,<sup>[28]</sup> 2,3,4,6-tetra-*O*-acetyl- $\alpha$ -D-glucopyranosyl bromide,<sup>[29]</sup> 1-methyl-3-(2,3,4,6-tetra-*O*-acetyl- $\beta$ -D-glucopyranosyl)imidazolium bromide<sup>[19]</sup> (magiHBr), and [magiAgBr]<sup>[19]</sup> were synthesized by the literature procedures.

**[1-Methyl-3-(2,3,4,6-tetra-*O*-acetyl- $\beta$ -D-glucopyranosyl)imidazol-2-yl]gold(I)chloride [magiAuCl]:** A solution of (tHt)AuCl (0.66 mmol) in CH<sub>2</sub>Cl<sub>2</sub> (4 mL) was added to a solution of [1-methyl-3-(2,3,4,6-tetra-*O*-acetyl- $\beta$ -D-glucopyranosyl)imidazol-2-yl]silver(I) bromide (magi)AgBr (0.66 mmol) in CH<sub>2</sub>Cl<sub>2</sub> (4 mL), and the mixture was stirred at room temperature overnight. After the removal of the insoluble solids by filtration through Celite®, the solution was concentrated, and diethyl ether was added to afford a white solid (yield 90 %). C<sub>18</sub>H<sub>24</sub>AuClN<sub>2</sub>O<sub>9</sub> (644.81): calcd. C 33.53, H 3.75, N 4.34; found C 33.50, H 3.73, N 4.31. <sup>1</sup>H NMR [400 MHz, (CD<sub>3</sub>)<sub>2</sub>SO, 298 K]:  $\delta$  = 7.80 (d, <sup>3</sup>*J*<sub>4'-H,5'-H</sub> = 2 Hz, 1 H, 4'-imidazolium), 7.51 (d, <sup>3</sup>*J*<sub>4'-H,5'-H</sub> = 2 Hz, 1 H, 5'-imidazolium), 6.22 (d, <sup>3</sup>*J*<sub>1-H,2-H</sub> = 8.8 Hz, 1 H, 1-H), 5.67 (t, <sup>3</sup>*J*<sub>3-H,2-H</sub> = 9.6 Hz, 1 H, 3-H), 5.46 (t, <sup>3</sup>*J*<sub>2-H,3-H</sub> = 9.6 Hz, 1 H, 2-H), 5.24 (t, <sup>3</sup>*J*<sub>3-H,4-H</sub> = 9.6 Hz, 1 H, 4-H), 4.37 (m, 1 H, 5-H), 4.32 (m, 2 H, 6-H), 4.17 (s, 3 H, CH<sub>3</sub>N), 2.10 (s, 3 H, AcO), 2.08 (s, 3 H, AcO), 2.06 (s, 3 H, AcO), 2.01 (s, 3 H, AcO) ppm. <sup>13</sup>C{<sup>1</sup>H} NMR [100 MHz, (CD<sub>3</sub>)<sub>2</sub>SO, 298 K]:  $\delta$  = 172.4 (2'-imidazolium), 170.1, 169.5, 169.4, 169.2, 123.8, 119.0, 84.8, 72.9, 71.6, 70.9, 67.5, 61.9, 37.9, 20.5, 20.4, 20.2, 20.4 ppm.

**[magiAuP1](BF<sub>4</sub>) and [magiAuP2](OSO<sub>2</sub>CF<sub>3</sub>):** A Schlenk tube was filled with magiAuCl (0.08 mmol) and PR<sub>3</sub> (0.085 mmol), which were dissolved in distilled dichloromethane (2 mL). The appropriate silver salt dissolved in methanol was added dropwise at room temperature. The reaction was continued for 1 h, during which a white precipitate appeared and then became grey after several minutes. After filtration through Celite®, the solution was concentrated, and diethyl ether was added to afford a white solid (yield 90 %).

**[magiAuP1]BF<sub>4</sub>:** C<sub>36</sub>H<sub>39</sub>AuBF<sub>4</sub>N<sub>2</sub>O<sub>9</sub>P (958.45): calcd. C 45.11, H 4.10, N 2.92; found C 44.97, H 3.98, N 2.88. <sup>1</sup>H NMR (500 MHz, CDCl<sub>3</sub>, 298 K): δ = 7.72–7.28 (m, 17 H), 5.86 (d, <sup>3</sup>J<sub>1-H,2-H</sub> = 9.5 Hz, 1 H, 1-H), 5.55 (t, <sup>3</sup>J<sub>2-H,3-H</sub> = 9.5 Hz, 1 H, 3-H), 5.40 (t, <sup>3</sup>J<sub>2-H,3-H</sub> = 9.5 Hz, 1 H, 2-H), 5.10 (t, <sup>3</sup>J<sub>3-H,4-H</sub> = 9.5 Hz, 1 H, 4-H), 4.19 (m, 1 H, 5-H), 4.08 (m, 1 H, 6-H), 4.02 (s, 3 H, CH<sub>3</sub>N), 4.0 (m, 1 H, 6'-H), 2.04 (s, 3 H, AcO), 1.99 (s, 3 H, AcO), 1.91 (s, 3 H, AcO), 1.84 (s, 3 H, AcO) ppm. <sup>19</sup>F{<sup>1</sup>H} NMR (376 MHz, CDCl<sub>3</sub>, 298 K): δ = 152.4 ppm. <sup>31</sup>P{<sup>1</sup>H} NMR (162 MHz, CDCl<sub>3</sub>, 298 K): δ = 40.3 ppm. <sup>13</sup>C{<sup>1</sup>H} NMR [100 MHz, (CD<sub>3</sub>)<sub>2</sub>SO, 298 K, selected data]: δ = 185.1 (2'-imidazolium), 170.6, 169.8, 169.5, 169.2, 124.1, 121.0, 86.4, 75.2, 73.0, 71.8, 67.9, 61.8, 39.4, 20.8, 20.7, 20.5, 20.4 ppm.

**[magiAuP2](OSO<sub>2</sub>CF<sub>3</sub>):** C<sub>58</sub>H<sub>59</sub>AuF<sub>3</sub>N<sub>3</sub>O<sub>18</sub>PS (1405.11): calcd. C 49.58, H 4.38, N 2.99; found C 50.03, H 4.72, N 2.87. <sup>1</sup>H NMR (400 MHz, CDCl<sub>3</sub>, 298 K): δ = 7.65–6.95 (m, 26 H), 6.09 (d, <sup>3</sup>J<sub>1-H,2-H</sub> = 12 Hz, 1 H, 1-H magi), 5.58 (s, 1 H, 7-H OP), 5.39 (t, <sup>3</sup>J<sub>2-H,3-H</sub> = <sup>3</sup>J<sub>3-H,4-H</sub> = 12 Hz, 1 H, 3-H magi), 5.16 (t, 1 H, 2-H magi), 5.11 (t, <sup>3</sup>J<sub>4-H,5-H</sub> = 12 Hz, 1 H, 4-H magi), 4.78 (d, <sup>3</sup>J<sub>1-H,2-H</sub> = 4 Hz, 1 H, 1-H OP), 4.40–4.48 (q AB, <sup>2</sup>J<sub>HA,HB</sub> = 12 Hz, 2 H, OCH<sub>2</sub>Ph), 4.30 (dd, <sup>3</sup>J<sub>2-H,3-H</sub> = 12 Hz, 1 H, 2-H OP), 4.22 (m, 1 H, 6-H magi), 4.19–4.13 (m, 2 H, 5-H, 6'-H magi), 4.11 (dd, <sup>2</sup>J<sub>6-H,6'-H</sub> = 4, <sup>3</sup>J<sub>6-H,5-H</sub> = 9.2 Hz, 1 H, 6-H OP), 4.05 (t, 1 H, 3-H OP), 3.98 (s, 3 H, CH<sub>3</sub>N), 3.87 (m, 1 H, 5-H OP), 3.72 (t, 1 H, 4-H OP), 3.52 (t, 1 H, 6'-H OP), 2.01 (s, 3 H, AcO), 2.0 (s, 3 H, AcO), 1.99 (s, 3 H, AcO), 1.97 (s, 3 H, AcO) ppm. <sup>13</sup>C{<sup>1</sup>H} NMR (100 MHz, CDCl<sub>3</sub>, 298 K, selected data): δ = 185.6 (2'-imidazolium), 170.6, 169.6, 169.4, 169.0, 168.4, 101.8, 97.0, 85.8, 80.8, 74.6, 72.4, 71.3, 68.7 (2), 67.4, 63.0, 61.2, 55.6, 38.9, 20.7, 20.5 (2), 20.0 ppm. <sup>19</sup>F{<sup>1</sup>H} NMR (376 MHz, CDCl<sub>3</sub>, 298 K): δ = -77.75 ppm. <sup>31</sup>P{<sup>1</sup>H} NMR (162 MHz, CDCl<sub>3</sub>): δ = 40.42 ppm.

**1-Methyl-3-(2,3,4,6-tetra-O-acetyl-β-D-glucopyranosyl)imidazolium Tetrafluoroborate (magiHBF<sub>4</sub>):** A round-bottomed flask was filled with magiHBr and NaBF<sub>4</sub> (0.65 mmol) in acetone (20 mL). The reaction was maintained at room temperature overnight. After the removal of the acetone under vacuum, the obtained white solid was partially dissolved in dichloromethane (30 mL), and filtration through paper afforded a colorless solution. The dichloromethane was then evaporated under vacuum to yield the pure product (98 % yield). C<sub>19</sub>H<sub>28</sub>BF<sub>4</sub>N<sub>2</sub>O<sub>9</sub> (515.24): calcd. C 44.29, H 5.48, N 5.44; found C 44.25, H 5.44, N 5.39. <sup>1</sup>H NMR (400 MHz, CDCl<sub>3</sub>, 298 K): δ = 9.55 (s, 1 H, 2'-imidazolium), 7.60 (bt, 1 H, 4'-imidazolium), 7.52 (bt, 1 H, 5'-imidazolium), 6.15 (d, <sup>3</sup>J<sub>1-H,2-H</sub> = 9.2 Hz, 1 H, 1-H), 5.43 (t, <sup>3</sup>J<sub>3-H,2-H</sub> = 9.6 Hz, 1 H, 3-H), 5.30 (t, <sup>3</sup>J<sub>2-H,1-H</sub> = 9.2 Hz, 1 H, 2-H), 5.23 (t, <sup>3</sup>J<sub>3-H,4-H</sub> = 9.6 Hz, 1 H, 4-H), 4.21 (m, 3 H), 4.03 (s, 3 H, CH<sub>3</sub>N), 2.05 (s, 3 H, AcO), 2.02 (s, 3 H, AcO), 1.98 (s, 3 H, AcO), 1.97 (s, 3 H, AcO) ppm. <sup>13</sup>C{<sup>1</sup>H} NMR (100 MHz, CDCl<sub>3</sub>, 298 K): δ = 170.8, 170.0, 169.9, 169.68, 137.3 (2'-imidazolium), 124.5, 120.0, 84.3, 75.0, 72.5, 70.6, 67.5, 61.6, 37.1, 20.8, 20.7, 20.6, 20.4 ppm. <sup>19</sup>F{<sup>1</sup>H} NMR (376 MHz, CD<sub>2</sub>Cl<sub>2</sub>, 298 K): δ = 150.6 ppm.

**{Bis[1-methyl-3-(2,3,4,6-tetra-O-acetyl-β-D-glucopyranosyl)imidazol-2-yl]}gold(II) Tetrafluoroborate [bis(magi)Au](BF<sub>4</sub>):** A round-bottomed flask was filled with magiHBF<sub>4</sub> (0.20 mmol), Ag<sub>2</sub>O (0.16 mmol), and molecular sieves 4 Å (MS 4 Å, 100 mg) in dichloromethane (12 mL). The reaction proceeded for 4 h at room temperature in the dark. Then, a solution of (tht)AuCl (0.10 mmol) in di-

chloromethane (3.4 mL) was added dropwise to the previous mixture, and the reaction proceeded overnight at room temperature in the dark. After filtration through Celite®, the volatiles were removed under vacuum to afford the product as a white solid (60 % yield). C<sub>36</sub>H<sub>48</sub>AuBF<sub>4</sub>N<sub>4</sub>O<sub>18</sub> (1108.55): calcd. C 39.00, H 4.36, N 5.05; found C 38.96, H 4.32, N 4.98. <sup>1</sup>H NMR [400 MHz, (CD<sub>3</sub>)<sub>2</sub>SO, 298 K]: δ = 7.87 (d, <sup>3</sup>J<sub>H,H</sub> = 1.6 Hz, 1 H, 4'-imidazolium), 7.62 (d, <sup>3</sup>J<sub>H,H</sub> = 1.6 Hz, 1 H, 5'-imidazolium), 6.29 (d, <sup>3</sup>J<sub>H,H</sub> = 8.4 Hz, 1 H, 1-H), 5.62 (t, <sup>3</sup>J<sub>H,H</sub> = 9.6 Hz, 1 H, 3-H), 5.57 (t, <sup>3</sup>J<sub>H,H</sub> = 9.6 Hz, 1 H, 2-H), 5.25 (t, <sup>3</sup>J<sub>H,H</sub> = 9.2 Hz, 1 H, 4-H), 4.37 (m, 1 H, 5-H), 4.32 (m, 2 H, 6-H), 3.95 (s, 3 H, CH<sub>3</sub>N), 2.05 (s, 3 H, AcO), 2.01 (s, 3 H, AcO), 1.99 (s, 3 H, AcO), 1.92 (s, 3 H, AcO) ppm. <sup>13</sup>C{<sup>1</sup>H} NMR [100 MHz, (CD<sub>3</sub>)<sub>2</sub>SO, 298 K]: δ = 182.9 (2'-imidazolium), 170.0, 169.5, 169.4, 168.7, 124.4, 119.6, 84.9, 73.2, 71.8, 70.6, 67.6, 61.9, 37.9, 20.5, 20.4, 20.2 ppm. <sup>19</sup>F{<sup>1</sup>H} NMR [376 MHz, (CD<sub>3</sub>)<sub>2</sub>SO<sub>2</sub>, 298 K]: δ = 148.2 ppm.

**X-ray Diffraction Analysis:** Colorless block-shaped single crystals of [magiAuCl] were obtained by the slow evaporation of a DMF solution at ambient temperature. A selected crystal was mounted in flowing N<sub>2</sub> at 173 K in a Bruker-Nonius KappaCCD diffractometer equipped with an Oxford Cryostream apparatus (graphite-monochromated Mo-K<sub>α</sub> radiation, λ = 0.71073 Å, CCD rotation images, thick slices, φ and ω scans to fill the asymmetric unit). Semiempirical absorption corrections (SADABS)<sup>[30]</sup> were applied. The structure was solved by direct methods (SIR97 program)<sup>[31]</sup> and refined anisotropically by the full-matrix least-squares method on F<sub>2</sub> against all independent measured reflections with SHELXL-2016/6 in the SHELX package.<sup>[32]</sup> All hydrogen atoms were introduced in calculated positions and refined in a riding model with U<sub>iso</sub>(H) equal to 1.2U<sub>eq</sub> or 1.5U<sub>eq</sub>(C<sub>methyl</sub>) of the carrier atom. The final refinements converged to R<sub>1</sub> = 0.0291 and wR<sub>2</sub> = 0.0773. DMF solvate molecules were present in the crystal. In the presence of strong anomalous scattered atoms, it was possible to determine the R/R/S/R/R absolute configuration at the five stereocenters C4/C5/C6/C7/C8, which agreed with that expected from the synthetic procedures. The figures were generated with the ORTEP-3<sup>[33]</sup> and Mercury CSD 3.3<sup>[34]</sup> programs.

CCDC 1548641 (for [magiAuCl]) contains the supplementary crystallographic data for this paper. These data can be obtained free of charge from The Cambridge Crystallographic Data Centre.

**Cell Culture:** Human prostate cancer cells (PC-3) were maintained in RPMI 1640 medium (GIBCO, USA), and human malignant melanoma cells (A375), human osteosarcoma cells (U2OS), and human breast carcinoma cells (MCF-7) were maintained in Dulbecco's modified Eagle's medium (DMEM; GIBCO, USA). Both media were supplemented with 10 % fetal bovine serum (GIBCO, USA) and 1 % L-glutamine (Lonza, Belgium) at 37 °C in a 5 % CO<sub>2</sub> humidified atmosphere and harvested at approximately 90 % confluence.

**Cell-Based Assays:** For cell growth studies, 4 × 10<sup>3</sup> cancer cells were seeded in 96-well flat-bottom microplates (50 μL of medium per well) and incubated overnight to allow cell adhesion. Subsequently, the culture medium was removed, and the cells were incubated with their growth medium (100 μL) with increasing concentrations of compound, appropriately diluted with dimethyl sulfoxide (DMSO), in quadruplicate for 72 h. The metabolic activities of cells was determined with a cell-counting kit 8 (CCK-8) assay, for which the instructions provided by the manufacture (Dojindo Lab, Japan) were followed. The CCK-8 solution (10 μL) was added directly to the culture wells, which were incubated for 2 h at 37 °C in a 5 % CO<sub>2</sub> humidified atmosphere. Finally, the absorbance was measured at λ = 450 nm with a microplate reader (Multiskan Fc 10094, Thermo). The reduction of the cell viability was determined by crystal violet assay. Shortly after treatment, the culture medium was removed,

and the cells were washed with phosphate-buffered saline (PBS) and then fixed and stained with 0.1 % (w/v) crystal violet in 25 % methanol for 30 min in the dark. The crystal violet was removed, and the cells were washed twice with double distilled water and left to dry. Then, the cells were solubilized by the addition of 10 % (v/v) acetic acid, and the amount of dye taken up was quantified with a plate reader at  $\lambda = 595$  nm. The  $EC_{50}$  values were calculated with the GraphPad Prism 5 software. The data were expressed as the mean  $\pm$  SD for three independent experiments.

**Lactate Dehydrogenase Assay:** The level of extracellular LDH released from damaged cells was measured as an indicator of the cytotoxicity. Cells ( $4 \times 10^3$ /well) was seeded in complete medium and treated with 1, 10, and 50  $\mu$ M [magiAuP1]BF<sub>4</sub> for 72 h. The cells were also treated with 0.1 % Triton X 100 as a positive control. Untreated cells were used as a negative control. The lysates and supernatant aliquots were then incubated with reaction buffer [0.7 mM *p*-iodonitrotetrazolium violet, 50 mM L-lactic acid, 0.3 mM phenazine methosulfate, 0.4 mM nicotinamide adenine dinucleotide (NAD), 0.2 M tris(hydroxymethyl)aminomethane hydrochloride (Tris/HCl) pH 8.0] for 30 min at 37 °C. The absorbance was read at  $\lambda = 490$  nm with a microplate reader (Thermo, Multiskan Fc). The percentage of LDH released was calculated as the absorbance in the medium of the treated cells divided by the absorbance in the medium of treated cells plus the absorbance in the total pellet of treated cells.

**Supporting Information** (see footnote on the first page of this article): X-ray crystallographic data.

## Acknowledgments

We would like to acknowledge F. De Luca Bossa and F. Ponticelli for their assistance with the synthetic procedures and we are also grateful to Prof. A. Casini for helpful discussion. A. D. thanks Diagnostica e Farmaceutica Molecolari S.C.R.L (DFM) for a grant. D. T. is indebted to the Inter-University Consortium for Research on the Chemistry of Metals in Biological Systems (CIRCMSB, Bari).

**Keywords:** Gold · Carbohydrates · Carbene ligands · Bioconjugation · Cytotoxicity

- [1] L. Kelland, *Nat. Rev. Cancer* **2007**, *7*, 573–84.
- [2] a) M. J. Clarke, F. Zhu, D. R. Frasca, *Chem. Rev.* **1999**, *99*, 2511–2533; b) S. Komeda, A. Casini, *Curr. Top. Med. Chem.* **2012**, *12*, 219–235.
- [3] a) E. M. Nagy, L. Ronconi, C. Nardon, D. Fregona, *Mini-Rev. Med. Chem.* **2012**, *12*, 1216–1229; b) L. Messori, A. Casini, *Curr. Top. Med. Chem.* **2011**, *11*, 2647–2660; c) I. Ott, *Coord. Chem. Rev.* **2009**, *253*, 1670–1681.
- [4] C. Roder, M. J. Thomson, *Drugs R&D* **2015**, *15*, 13–20.
- [5] <https://clinicaltrials.gov/ct2/show/NCT01747798>.
- [6] C. K. Mirabelli, R. K. Johnson, D. T. Hill, L. F. Faucette, G. R. Girard, G. Y. Kuo, C. M. Sung, S. T. Crooket, *J. Med. Chem.* **1986**, *29*, 218–223.
- [7] a) A. Gutiérrez, L. Gracia-Fleta, I. Marzo, C. Cativiela, A. Laguna, M. C. Gimeno, *Dalton Trans.* **2014**, *43*, 17054–17066; b) H. Goitia, Y. Nieto, M. D. Villacampa, C. Kasper, A. Laguna, M. C. Gimeno, *Organometallics* **2013**, *32*, 6069–6078; c) A. Gutiérrez, I. Marzo, C. Cativiela, A. Laguna, M. C. Gimeno, *Chem. Eur. J.* **2015**, *21*, 11088–11095.
- [8] a) M. V. Baker, P. J. Barnard, S. J. Berners-Price, S. K. Brayshaw, J. L. Hickey, B. W. Skelton, A. H. White, *J. Organomet. Chem.* **2005**, *690*, 5625–5635; b) W. Liu, R. Gust, *Chem. Soc. Rev.* **2013**, *42*, 755–773; c) H. G. Raubenheimer, S. Cronje, *Chem. Soc. Rev.* **2008**, *37*, 1998–2011.
- [9] For representative examples, see: a) M. V. Baker, P. J. Barnard, S. J. Berners-Price, S. K. Brayshaw, J. L. Hickey, B. W. Skelton, A. H. White, *Dalton Trans.* **2006**, 3708–3715; b) L. Messori, C. Gabbiani, “Recent Trends in Antitumor gold(III) Complexes: Innovative Cytotoxic Metalodrugs for Cancer Treatment” in *Metal Compounds in Cancer Chemotherapy* (Eds.: J. M. Pérez, M. A. Fuertes C. Alonso), Research Signpost, Kerala, **2005**, pp. 355–375; c) C. A. Tessier, C. L. Cannon, W. J. Youngs, *Chem. Rev.* **2009**, *109*, 3859–3884; d) R. Rubbiani, S. Can, I. Kitanovic, H. Alborzina, M. Stefanopoulou, M. Kokoschka, S. Mönchgesang, W. S. Sheldrick, S. Wölfl, I. Ott, *J. Med. Chem.* **2011**, *54*, 8646–8657; e) F. Cisnetti, A. Gautier, *Angew. Chem. Int. Ed.* **2013**, *52*, 11976–11978; *Angew. Chem.* **2013**, *125*, 12194; f) C. Hu, X. Li, W. Wang, R. Zhang, L. Deng, *Curr. Med. Chem.* **2014**, *21*, 1220–1230; g) A. Gutiérrez, M. C. Gimeno, I. Marzo, N. Metzler-Nolte, *Eur. J. Inorg. Chem.* **2014**, 2512–2519; h) R. Visbal, V. Fernández-Moreira, I. Marzo, A. Laguna, M. C. Gimeno, *Dalton Trans.* **2016**, *45*, 15026–15033.
- [10] For representative examples, see: a) J. Weaver, S. Gaillard, C. Toye, S. Macpherson, S. P. Nolan, A. Riches, *Chem. Eur. J.* **2011**, *17*, 6620–6624; b) L. Messori, L. Marchetti, L. Massai, F. Scaletti, A. Guerri, I. Landini, S. Nobili, G. Perrone, E. Mini, P. Leoni, M. Pasquali, C. Gabbiani, *Inorg. Chem.* **2014**, *53*, 2396–2403; c) X. Cheng, P. Holenya, S. Can, H. Alborzina, R. Rubbiani, I. Ott, S. Wölfl, *Mol. Cancer* **2014**, *13*, 221; d) M. Tacke, *J. Organomet. Chem.* **2015**, *782*, 17–21; e) E. García-Moreno, S. Gascón, J. A. García de Jalón, E. Romanos, M. J. Rodríguez-Yoldi, M. Laguna, *Anti-Cancer Agents Med. Chem.* **2015**, *15*, 773–782; f) B. Bertrand, A. Casini, *Dalton Trans.* **2014**, *43*, 4209–4219.
- [11] a) J. L. Hickey, R. A. Ruhayel, P. J. Barnard, M. V. Baker, S. J. Berners-Price, A. J. Filipovska, *J. Am. Chem. Soc.* **2008**, *130*, 12570–12571; b) P. J. Barnard, S. J. Berners-Price, *Coord. Chem. Rev.* **2007**, *251*, 1889–1902; c) A. Bindoli, M. P. Rigobello, G. Scutari, C. Gabbiani, A. Casini, L. Messori, *Coord. Chem. Rev.* **2009**, *253*, 1692–1707; d) A. Pratesi, C. Gabbiani, E. Michelucci, M. Ginanneschi, A. M. Papini, R. Rubbiani, I. Ott, L. Messori, *J. Inorg. Biochem.* **2014**, *136*, 161–169.
- [12] a) K. P. Bhabak, B. J. Bhuyan, G. Magesh, *Dalton Trans.* **2011**, *40*, 2099–2111; b) D. Krishnamurthy, M. R. Karver, E. Fiorillo, V. Orru, S. M. Stanford, N. Bottini, A. M. Barrios, *J. Med. Chem.* **2008**, *51*, 4790–4795; c) C. Gabbiani, F. Scaletti, L. Massai, E. Michelucci, M. Cinellu, L. Messori, *Chem. Commun.* **2012**, *48*, 11623–11625.
- [13] G. Ferraro, C. Gabbiani, A. Merlino, *Bioconjugate Chem.* **2016**, *27*, 1584–1587.
- [14] a) B. Bertrand, L. Stefan, M. Pirrotta, D. Monchaud, E. Bodio, P. Richard, P. Le Gendre, E. Warmerdam, M. H. de Jager, G. M. M. Groothuis, M. Picquet, A. Casini, *Inorg. Chem.* **2014**, *53*, 2296–2303; b) C. V. Maftai, E. Fodor, P. G. Jones, M. Freytag, M. H. Franz, G. Kelter, H. H. Fiebig, M. Tamm, I. Neda, *Eur. J. Med. Chem.* **2015**, *101*, 431–445.
- [15] W. Niu, X. Chen, W. Tan, A. S. Veige, *Angew. Chem. Int. Ed.* **2016**, *55*, 8889–8893; *Angew. Chem.* **2016**, *128*, 9035.
- [16] a) M. G. Vander Heiden, L. C. Cantley, C. B. Thompson, *Science* **2009**, *324*, 1029–1033; b) O. Warburg, *Science* **1956**, *123*, 309–314; c) Q. Wang, Z. Huang, J. Ma, X. Lu, L. Zhang, X. Wang, P. G. Wang, *Dalton Trans.* **2016**, *45*, 10366–10374.
- [17] T. Storr (Ed.), *Ligand Design in Medicinal Inorganic Chemistry*, John Wiley & Sons, Chichester, **2014**.
- [18] V. Benessere, M. Lega, F. Ruffo, *J. Organomet. Chem.* **2014**, *771*, 105–116 and references cited therein.
- [19] T. Nishioka, T. Shibata, I. Kinoshita, *Organometallics* **2007**, *26*, 1126–1128.
- [20] B. Bertrand, E. Bodio, P. Richard, M. Picquet, P. Le Gendre, A. Casini, *J. Organomet. Chem.* **2015**, *775*, 124–129.
- [21] a) P. de Fremont, N. M. Scott, E. D. Stevens, S. P. Nolan, *Organometallics* **2005**, *24*, 2411–2418; b) see ref.<sup>[8a]</sup>
- [22] V. Benessere, F. Ruffo, *Tetrahedron: Asymmetry* **2010**, *21*, 171–176.
- [23] W. Liu, K. Benschdorf, M. Proetto, U. Abram, A. Hagenbach, R. Gust, *J. Med. Chem.* **2011**, *54*, 8605–8615.
- [24] I. J. B. Lin, C. S. Vasam, *Can. J. Chem.* **2005**, *83*, 812–825.
- [25] W. Liu, K. Benschdorf, M. Proetto, A. Hagenbach, U. Abram, R. Gust, *J. Med. Chem.* **2012**, *55*, 3713–3724.
- [26] The inertness of [bis(magi)Au][BF<sub>4</sub>] was confirmed with several cancer cell lines (data not show).
- [27] R. Weinlich, A. Oberst, H. M. Beere, D. R. Green, *Nat. Rev. Mol. Cell Biol.* **2017**, *18*, 127–136.
- [28] R. Uson, A. Laguna, M. Laguna, *Inorg. Synth.* **1989**, *26*, 85–91.
- [29] W. A. Szarek, O. Achmatowicz, J. Plenkiwicz, B. K. Radatus, *Tetrahedron* **1978**, *34*, 1427–1433.

- [30] SADABS, Bruker-Nonius, Delft, **2002**.
- [31] A. Altomare, M. C. Burla, M. Camalli, G. L. Cascarano, C. Giacovazzo, A. Guagliardi, A. G. G. Moliterni, G. Polidori, R. Spagna, *J. Appl. Crystallogr.* **1999**, *32*, 115–119.
- [32] G. M. Sheldrick, *Acta Crystallogr., Sect. C: Cryst. Struct. Commun.* **2015**, *71*, 3–8.
- [33] L. J. Farrugia, *J. Appl. Crystallogr.* **1997**, *30*, 565–566.
- [34] C. F. Macrae, P. R. Edgington, P. McCabe, E. Pidcock, G. P. Shields, R. Taylor, M. Towler, J. van der Streek, *J. Appl. Crystallogr.* **2006**, *39*, 453–457.

---

Received: June 28, 2017